Math. Control Signals Syst. (2013) 25:37–61
DOI 10.1007/s00498-012-0091-1

ORIGINAL ARTICLE

Semi-classical signal analysis

Taous-Meriem Laleg-Kirati · Emmanuelle Crépeau · Michel Sorine

Received: 18 June 2010 / Accepted: 22 August 2012 / Published online: 30 September 2012
© Springer-Verlag London Limited 2012

Abstract This study introduces a new signal analysis method, based on a semi-classical approach. The main idea in this method is to interpret a pulse-shaped signal as a potential of a Schrödinger operator and then to use the discrete spectrum of this operator for the analysis of the signal. We present some numerical examples and the first results obtained with this method on the analysis of arterial blood pressure waveforms.

Keywords Signal analysis · Schrödinger operator · Semi-classical · Arterial blood pressure

1 Introduction

In this paper, we consider a signal, usually represented by a real-valued function $y(t)$, $t \in \mathbb{R}$ and introduce a new method to analyze this signal. The main idea in this method is, under some assumptions given below, to interpret the signal y as a multiplication operator, $\phi \to y \cdot \phi$, on some function space. The spectrum of a (formally) regularized version of this operator, denoted $H_h(y)$ and defined by

T.-M. Laleg-Kirati (✉)
Computer, Electrical and Mathematical Sciences and Engineering Division (CEMSE),
King Abduallah University of Science and Technology (KAUST),
Thuwal, Kingdom of Saudi Arabia
e-mail: taousmeriem.laleg@kaust.edu.sa

E. Crépeau
Versailles Saint Quentin en Yvelines University, Bât Fermat, 78035 Versailles Cedex, France

M. Sorine
Centre Paris, Rocquencourt, INRIA, Domaine de Voluceau, BP 105, 78153 Le Chesnay Cedex, France

$$H_h(y)\psi(t) = -h^2\frac{d^2\psi(t)}{dt^2} - y(t)\psi(t), \quad \psi \in H^2(\mathbb{R}), \quad h > 0, \tag{1}$$

for small h, is then used for the analysis instead of the Fourier transform of y. Here $H^2(\mathbb{R})$ denotes the Sobolev space of order 2. In this method, the signal is interpreted as a potential of a Schrödinger operator. This point of view seems useful when associated inverse spectral problem is well posed as it will be the case for some pulse-shaped signals.

We suppose that y is a real-valued function and we define H_h on a space $\mathcal{B}$ such that

$$\mathcal{B} = \left\{ y \in L_1^1(\mathbb{R}), \quad y(t) \geq 0, \quad \forall t \in \mathbb{R}, \quad \frac{\partial^m y}{\partial t^m} \in L^1(\mathbb{R}), \quad m = 1, 2 \right\}, \tag{2}$$

with, $L_1^1(\mathbb{R}) = \{V | \int_{-\infty}^{+\infty} |V(t)|(1 + |t|)dt < \infty\}$. $L_1^1(\mathbb{R})$ is known as the Faddeev class [9].

For $\lambda \leq 0$, we denote $N_h(\lambda; y)$ the number of eigenvalues of the operator $H_h(y)$ below λ. Under hypothesis (2), there is a non-zero finite number $N_h = N_h(0; y)$, as it is described in Proposition 1. We denote $-\kappa_{nh}^2$ the negative eigenvalues of $H_h(y)$ with $\kappa_{nh} > 0$ and $\kappa_{1h} > \kappa_{2h} > \cdots > \kappa_{nh}$, $n = 1, \ldots, N_h$. Let ψ_{nh}, $n = 1, \ldots, N_h$ be the associated L^2-normalized eigenfunctions.

In this study, we focus our interest in representing the signal y with the discrete spectrum of $H_h(y)$ using the following formula (3)

$$y_h(t) = 4h \sum_{n=1}^{N_h} \kappa_{nh} \psi_{nh}^2(t), \qquad x \in \mathbb{R}. \tag{3}$$

As we will see, the parameter h plays an important role in our approach. Indeed, the approximation $|y - y_h|$ improves as h decreases. We will be especially interested in the asymptotic properties of the method when h goes to 0. Therefore, the method is based on semi-classical concepts. Indeed "semi-classical" is a concept used in quantum mechanics to deign the fact that the actions of the studied system are large comparing to the quantum h. In mathematics, this property can be interpreted as the asymptotic expansions of the actions in a neighborhood of $h = 0$. We will call it semi-classical signal analysis (SCSA).

In the next section, we will present some properties of the SCSA. In Sect. 3, we will consider a particular case of an exact representation for a fixed h and show its relation to a signal representation using the so-called reflectionless potentials of the Schrödinger operator. Section 4 will deal with some numerical examples and Sect. 5 will present some results obtained on the analysis of arterial blood pressure (ABP) signals using the SCSA. A discussion will summarize the main results and compare the SCSA to related studies. In Appendices Appendix A:, Appendix B: and Appendix C: some known results on direct and inverse scattering transforms are presented.

2 SCSA properties

To begin, we focuss our attention on the behavior of the number N_h of negative eigenvalues of $H_h(y)$ according to h as described by the following proposition.

Proposition 1 *Let y be a real-valued function satisfying hypothesis (2). Then,*
(i) The number N_h of negative eigenvalues of $H_h(y)$ is a decreasing function of h.
(ii) Moreover if $y \in L^{\frac{1}{2}}(\mathbb{R})$, then,

$$\lim_{h\to 0} hN_h = \frac{1}{\pi}\int_{-\infty}^{+\infty} \sqrt{y(t)}dt, \tag{4}$$

Proof (i) The proof of this item is based on the following lemma.

Lemma 1 [2,28] *For $\lambda \leq 0$, let $N_1(\lambda; V)$ be the number of negative eigenvalues of $H_1(V)$ less than λ. Let $V(t)$ and $W(t)$ be two potentials of the Schrödinger operator such that $W(t) \leq V(t)$, $\forall t$ then*

$$N_1(\lambda; W) \leq N_1(\lambda; V), \quad \forall \lambda \leq 0. \tag{5}$$

Let $y(t) \in \mathcal{B}$. We put $V(t) = \frac{1}{h_1^2}y(t)$, $W(t) = \frac{1}{h_2^2}y(t)$, with $0 < h_1 \leq h_2$.

For $\lambda = 0$, we obtain $N_1(0; \frac{1}{h_2^2}y) \leq N_1(0; \frac{1}{h_1^2}y)$, and we have $N_1(0; \frac{1}{h_j^2}y) = N_{h_j}$, $j = 1, 2$, which proves the result.

(ii) Let $y \in \mathcal{B} \cap L^{\frac{1}{2}}(\mathbb{R})$ and $\lambda \in]-y_{\max}, 0]$. We denote

$$S_\gamma(h, \lambda) = \sum_{\kappa_{nh}^2 \leq \lambda} \left(\lambda + \kappa_{nh}^2\right)^\gamma, \qquad \gamma \geq 0 \tag{6}$$

the Riesz means of the values $-\kappa_{nh}^2$ less than λ. Remark that $S_0(h, \lambda) = N_h(\lambda; y)$.

Property (ii) results from the following Lemma 2.

Lemma 2 [23] *For $y \in L^{\gamma+\frac{1}{2}}(\mathbb{R})$, $y(t) \geq 0$, $\forall x \in \mathbb{R}$ and $\gamma \geq 0$, we have*

$$\lim_{h\to 0} hS_\gamma(h, 0) = L_\gamma^{cl}\int_{-\infty}^{+\infty} y(t)^{\gamma+\frac{1}{2}}dt, \tag{7}$$

where L_γ^{cl} is the classical constant given by

$$L_\gamma^{cl} = \frac{\Gamma(\gamma+1)}{2\sqrt{\pi}\Gamma(\gamma+\frac{3}{2})}, \tag{8}$$

for all $\gamma \geq 0$

By taking $\gamma = 0$ in (7) we get the result.

Let us now study some properties of the negative eigenvalues $-\kappa_{nh}^2, n = 1, \ldots, N_h$ of $H_h(y)$.

Proposition 2 *Let $y \in C^\infty(\mathbb{R})$, with $y(t) > 0$, $\forall x \in \mathbb{R}$ and such that $\exists \gamma_0 \in \mathbb{R}$, $\min_{\mathbb{R}}(-y + \gamma_0) > 0$ and $\forall \alpha \in \mathbb{N}$, $\exists C_\alpha > 0$ such that $|\frac{\partial^\alpha y}{\partial t^\alpha}| \leq C_\alpha(-y + \gamma_0)$, then*

every regular value of y is an accumulation point of the set $(\kappa_{nh}^2, n = 1, \ldots, N_h)$ (v is a regular value if $0 < v < y_{\max}$ and if $y(t) = v$ then $|\frac{dy(t)}{dt}| > 0$).

Proof We want to show that every regular value of y is an accumulation point for the set $(\kappa_{nh}^2, n = 1, \ldots, N_h)$. For this purpose, we use the following result shown by Helffer and Robert [14].

Theorem 1 [14] *Let $y \in C^\infty(\mathbb{R})$, with $y(t) > 0$, $\forall x \in \mathbb{R}$ such that for $\gamma_0 \in \mathbb{R}$, $\min_{\mathbb{R}}(-y + \gamma_0) > 0$ and for all $\alpha \in \mathbb{N}$, there is a constant $C_\alpha > 0$ such that $|\frac{\partial^\alpha y}{\partial x^\alpha}| \leq C_\alpha(-y + \gamma_0)$. Let $\lambda < \liminf_{|t|\to\infty}(-y(t))$, then for $0 \leq \gamma \leq 1$ the Riesz means (6) are given by*

$$S_\gamma(h, \lambda) = \frac{1}{h}\left(L_\gamma^{cl} \int_{-\infty}^{+\infty} |\lambda + y(t)|_+^{\gamma+\frac{1}{2}}\, dt + O(h^{1+\gamma})\right), \tag{9}$$

where $|V|_+$ is the positive part of V and L_γ^{cl}, known as the classical constant, is given by (8).

We put $\gamma = 0$ in (6). We notice that $S_0(h, \lambda) = N_h(\lambda, y)$. Substituting γ by 0 in (9), we get

$$S_0(h, \lambda) = \frac{1}{h} L_0^{cl} \int_{-\infty}^{+\infty} \sqrt{|\lambda + y(t)|_+}\, dt + O(1). \tag{10}$$

We suppose that there is a regular value y_0 of y that is not an accumulation point of the set $(\kappa_{nh}^2, n = 1, \ldots, N_h)$. So there is a neighborhood $V(y_0)$ of y_0 and a value h_0, small enough such that $\forall h < h_0$, $V(y_0)$ does not contain any element element κ_{nh}^2.

Moreover, we can choose $V(y_0)$ small enough such that

$$\inf\left\{\left|\frac{dy(t)}{dt}\right|, \quad \text{for} \quad t \quad \text{such that} \quad y(t) \in V(y_0)\right\} = c > 0. \tag{11}$$

Then, we can take $V(y_0) = [y_1, y_2[$, with y_1 and y_2 some regular values of y and $0 < y_1 < y_2$.

For all $h < h_0$, the difference $S_0(h, -y_1) - S_0(h, -y_2)$ represents the number of elements of $(-\kappa_{nh}^2, n = 1, \ldots, N_h)$ in the interval $]-y_2, -y_1]$. However, this set is empty because there is no element in the neighborhood of y_0.

Denoting $T(\lambda) = \{t | y(t) + \lambda \geq 0\}$, we have from (10)

$$S_0(h, -y_1) - S_0(h, -y_2) = \frac{1}{h} L_0^{cl}\left(\int_{T(-y_1)} \sqrt{y(t) - y_1}\, dt - \int_{T(-y_2)} \sqrt{y(t) - y_2}\, dt\right) + O(1), \tag{12}$$

so, as the left quantity is null, we obtain

$$\int_{T(-y_1)} \sqrt{y(t)-y_1}dt = \int_{T(-y_2)} \sqrt{y(t)-y_2}dt, \tag{13}$$

and we have $T(-y_1) = T(-y_2) \cup y^{-1}([y_1, y_2[)$, so

$$\int_{T(-y_2)} \sqrt{y(t)-y_1}dt + \int_{y^{-1}([y_1,y_2[)} \sqrt{y(t)-y_1}dt = \int_{T(-y_2)} \sqrt{y(t)-y_2}dt, \tag{14}$$

$$\int_{T(-y_2)} (\sqrt{y(t)-y_1} - \sqrt{y(t)-y_2})dt + \int_{y^{-1}([y_1,y_2[)} \sqrt{y(t)-y_1}dt = 0. \tag{15}$$

Hence as these two integrals are positives, we get

$$\int_{y^{-1}([y_1,y_2[)} \sqrt{y(t)-y_1}dt = 0, \tag{16}$$

therefore $|y(t) - y_1| = 0$ almost everywhere in $y^{-1}([y_1, y_2[)$, then $y_1 = y_2$, which is a contradiction.

Now, Proposition 2 introduces an interesting property of the SCSA. Indeed, remembering that

$$-h^2\frac{d^2\psi_{nh}(t)}{dt^2} - y(t)\psi_{nh}(t) = -\kappa_{nh}^2\psi_{nh}(t). \tag{17}$$

and by multiplying the previous equation by $\psi_{nh}(t)$ and integrating it by part, we get

$$\kappa_{nh}^2 = \int_{-\infty}^{+\infty} y\psi_{nh}^2(t)dt - h^2\int_{-\infty}^{+\infty}\left(\frac{d\psi_{nh}(t)}{dt}\right)^2 dt. \tag{18}$$

Then, we notice that $-y_{\max} \leq -\kappa_{nh}^2 < 0$ as it is illustrated in Fig. 1. Hence, for a fixed value of h, κ_{nh}^2 can be interpreted as particular values of y which define a new quantization approach that can be interpreted by semi-classical concepts. The SCSA appears then as a new way to quantify a signal.

To finish this section, we examine the convergence of the first two momentums of κ_{nh} when $h \to 0$ through Proposition 3. These quantities could be very interesting in signal analysis as it is mentioned in Sect. 5 and also in a recent study [20].

Proposition 3 *Under hypothesis* (2)*, we have*

$$\lim_{h\to 0} h\sum_{n=1}^{N_h}\kappa_{nh} = \frac{1}{4}\int_{-\infty}^{+\infty} y(t)dt, \tag{19}$$

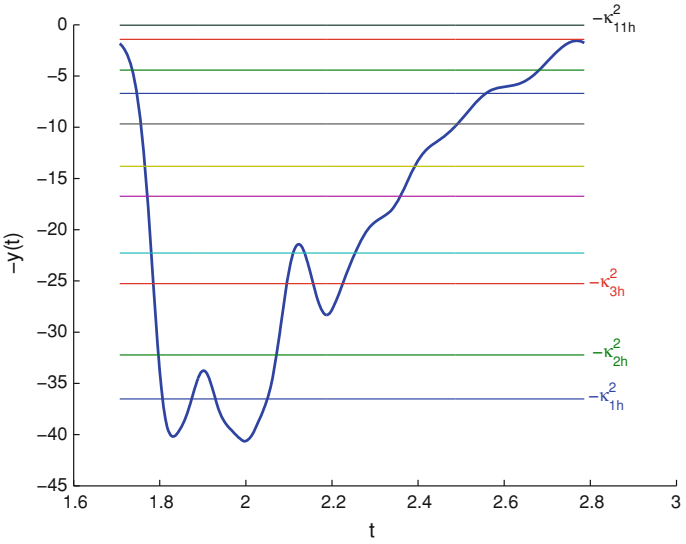

Fig. 1 The negative spectrum of the Schrödinger operator $-h^2\frac{d^2}{dt^2} - y(t)$ provides a quantization of the signal y

and remembering that

$$y_h(t) = 4h\sum_{n=1}^{N_h}\kappa_{nh}\psi^2_{nh}(t), \qquad t \in \mathbb{R}, \tag{20}$$

we have

$$\lim_{h\to 0} h\int_{-\infty}^{+\infty} y_h(t)dt = \int_{-\infty}^{+\infty} y(t)dt. \tag{21}$$

Moreover if $y \in L^2(\mathbb{R})$, then,

$$\lim_{h\to 0} h\sum_{n=1}^{N_h}\kappa^3_{nh} = \frac{3}{16}\int_{-\infty}^{+\infty} y^2(t)dt. \tag{22}$$

Proof The limits (19) and (22) are deduced from Lemma 2 for $\gamma = \frac{1}{2}$ and $\gamma = \frac{3}{2}$ respectively,

$$\lim_{h\to 0} h\sum_{n=1}^{N_h}\kappa_{nh} = \frac{1}{4}\int_{-\infty}^{+\infty} y(t)dt, \tag{23}$$

$$\lim_{h\to 0} h\sum_{n=1}^{N_h}\kappa^3_{nh} = \frac{3}{16}\int_{-\infty}^{+\infty} y^2(t)dt. \tag{24}$$

By integrating (3) we have

$$\int_{-\infty}^{+\infty} y_h(t)dt = 4h\sum_{n=1}^{N_h}\kappa_{nh}. \tag{25}$$

Then, combining (25) and (19), we get (21).

3 Exact representation and reflectionless potentials

In this section, we are interested in an exact representation of a signal for a fixed h and its relation to reflectionless potentials (reflectionless potentials are defined in the Appendix Appendix B:) of the Schrödinger operator as it is described in the following proposition:

Proposition 4 *The following properties are equivalent:*

(i) *Equality in (19) holds for a finite h;*
(ii) $\exists h$ *such that* $y_h = y$;
(iii) $\exists h$ *such that* $\frac{y}{h^2}$ *is a reflectionless potential of* $H_1(V)$.

Proof The following proof uses some concepts and results from scattering transform theory that are recalled in the appendix. First, we suppose that (i) is fulfilled then

$$\exists h,\quad \int_{-\infty}^{+\infty} y(t)dt = 4h\sum_{n=1}^{N_h}\kappa_{nh}. \tag{26}$$

Writing the first invariant (56) (see the Appendix Appendix C:) for the potential $-\frac{y}{h^2}$, we have

$$\int_{-\infty}^{+\infty} y(t)dt = 4h\sum_{n=1}^{N_h}\kappa_{nh} + \frac{h^2}{\pi}\int_{-\infty}^{+\infty}\ln\left(1-|R_{r(l)h}(k)|^2\right)dk, \tag{27}$$

where $R_{r(l)h}(k)$ is the reflection coefficient (see the Appendix Appendix A:).

Using (25), we get

$$\int_{-\infty}^{+\infty} y(t)dt = \int_{-\infty}^{+\infty} y_h(t)dt + \frac{h^2}{\pi}\int_{-\infty}^{+\infty}\ln\left(1-|R_{r(l)h}(k)|^2\right)dk. \tag{28}$$

Then, from (30) and (28) we obtain

$$\int_{-\infty}^{+\infty}\ln\left(1-|R_{r(l)h}(k)|^2\right)dk = 0. \tag{29}$$

The reflection coefficient of a Schrödinger operator satisfies $|R_{r(l)h}(k)| \leq 1, \forall k \in \mathbb{R}$ (see for example [6]). Then, we get $\ln(1 - |R_{r(l)h}(k)|^2) \leq 0$. Equality (29) is then fulfilled if and only if $\ln(1 - |R_{r(l)h}(k)|^2) = 0$, $k \in \mathbb{R}$ a.e; which is true only if $|R_{r(l)h}(k)| = 0$, $k \in \mathbb{R}$ a.e. This property defines a reflectionless potential. So, $(i) \Rightarrow (iii)$.

Now, using the Deift-Trubowitz formula (52) (see Appendix Appendix B:) that we rewrite for the potential $-\frac{y}{h^2}$ and taking $R_{r(l)h}(k) = 0$, we can deduce that statement (iii) implies statement (ii).

Then, if we suppose that $y_h = y$ for a given value of h we have

$$\int_{-\infty}^{+\infty} y_h(t)dt = \int_{-\infty}^{+\infty} y(t)dt, \tag{30}$$

hence $(ii) \Rightarrow (i)$

4 Numerical results

In this section, we are interested in the validation of the SCSA through some numerical examples. For this purpose, it will be more convenient to consider the problem associated to $H_1(\frac{y}{h^2})$. Therefore, in order to simplify the notations, we put $\frac{1}{h^2} = \chi$, $N_h = N_\chi$ and $\frac{\kappa_{nh}^2}{h^2} = \kappa_{n\chi}^2$, $n = 1, \ldots, N_\chi$. We denote the L^2-normalized eigenfunctions $\psi_{n\chi}$, $n = 1, \ldots, N_\chi$. Formula (3) is then rewritten

$$y_\chi(t) = \frac{4}{\chi} \sum_{n=1}^{N_\chi} \kappa_{n\chi} \psi_{n\chi}^2(t), \qquad x \in \mathbb{R}, \tag{31}$$

We start by giving the numerical scheme used to estimate a signal with the SCSA. Then, the sech-squared function will be considered. This example illustrates the influence of the parameter χ on the approximation. Gaussian, sinusoidal and chirp signals will be also considered.

4.1 The numerical scheme

The first step in the SCSA is to solve the spectral problem of a one-dimensional Schrödinger operator. Its discretization leads to an eigenvalue problem of a matrix. In this work, we propose to use a Fourier pseudo-spectral method [15,30]. The latter is well-adapted for periodic problems but in practice it gives good results for some non-periodic problems, for instance, rapid decreasing signals.

We consider a grid of M equidistant points t_j, $j = 1, \ldots, M$ such that

$$a = t_1 < t_2 < \cdots < t_{M-1} < t_M = b. \tag{32}$$

Let $\Delta t = \dfrac{b-a}{M-1}$ be the distance between two consecutive points. We denote y_j and ψ_j the values of y and ψ at the grid points t_j, $j = 1, \ldots, M$

$$y_j = y(t_j), \quad \psi_j = \psi(t_j), \quad j = 1, \ldots, M. \tag{33}$$

Therefore, the discretization of the Schrödinger eigenvalue problem leads to the following eigenvalue matrix problem

$$(-\boldsymbol{D}_2 - \chi \operatorname{diag}(\boldsymbol{Y}))\,\underline{\boldsymbol{\psi}} = \lambda \underline{\boldsymbol{\psi}}, \tag{34}$$

where $\operatorname{diag}(\boldsymbol{Y})$ is a diagonal matrix whose elements are y_j, $j = 1, \ldots, M$ and $\underline{\boldsymbol{\psi}} = \begin{bmatrix}\psi_1 & \psi_2 & \cdots & \psi_{M-1} & \psi_M\end{bmatrix}^T$. D_2 is the second order differentiation matrix given by [30],

– If M is even

$$\boldsymbol{D}_2(k,j) = \frac{\Delta^2}{(\Delta t)^2} \begin{cases} \dfrac{-\pi^2}{3\Delta^2} - \dfrac{1}{6} & \text{for } k = j, \\ -(-1)^{k-j}\,\dfrac{1}{2}\,\dfrac{1}{\sin^2\left(\frac{(k-j)\Delta}{2}\right)} & \text{for } k \neq j. \end{cases} \tag{35}$$

– If M is odd

$$\boldsymbol{D}_2(k,j) = \frac{\Delta^2}{(\Delta t)^2} \begin{cases} \dfrac{-\pi^2}{3\Delta^2} - \dfrac{1}{12} & \text{pour } k = j, \\ -(-1)^{k-j}\,\dfrac{1}{2}\,\dfrac{1}{\sin\left(\frac{(k-j)\Delta}{2}\right)}\cot\left(\frac{(k-j)\Delta}{2}\right) & \text{pour } k \neq j, \end{cases} \tag{36}$$

with $\Delta = \dfrac{2\pi}{M}$, the matrix $\boldsymbol{D}_2$ is symmetric and definite negative. To solve the eigenvalue problem of the matrix $(-\boldsymbol{D}_2 - \chi \operatorname{diag}(\boldsymbol{Y}))$ we use the Matlab routine eig.

The final step in the SCSA algorithm is to find an optimal value of the parameter χ. So we look for a value $\hat{\chi}$ that gives a good approximation of y with a small number of negative eigenvalues. From the numerical tests, we noticed that the number N_χ is in general a step-by-step function of χ. So, we optimize the following criteria in each interval $[\chi_1, \chi_2]$ where N_χ is constant,

$$J(\chi) = \frac{1}{M}\sum_{i=1}^{M}\left(y_i - y_{\chi i}\right)^2, \quad y_{\chi i} = \frac{4}{\chi}\sum_{n=1}^{N_\chi}\kappa_{n\chi}\,\psi_{ni\chi}^2, \quad i = 1, \ldots, M. \tag{37}$$

For χ large enough (equivalently h small enough), we know an approximate relation between the number of negative eigenvalues and χ thanks to Proposition 1.

Then, we can deduce approximate values of χ_1 and χ_2 according to a given number of negative eigenvalues. Figure 2 summarizes the SCSA algorithm.

Remark 1 In practice, we often omit the optimization step and just fix N_χ to a large enough value.

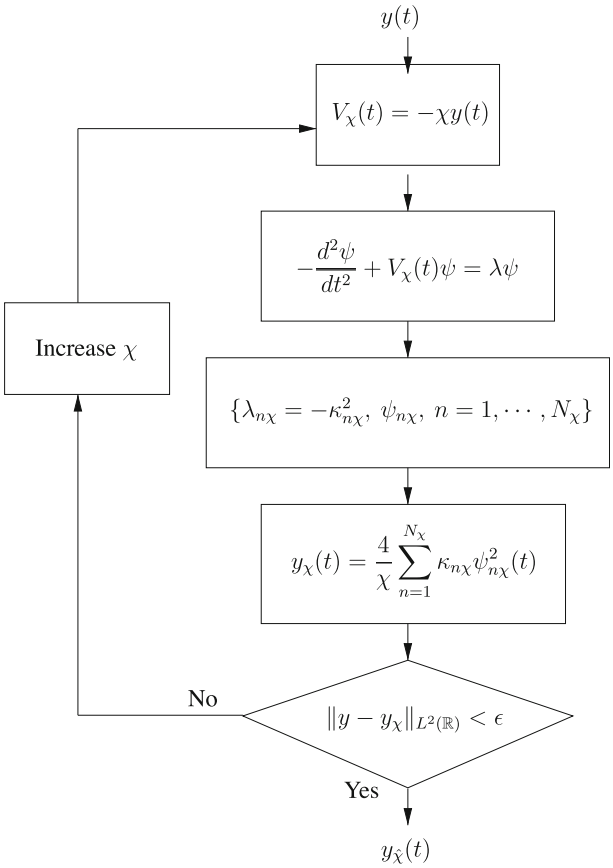

Fig. 2 The SCSA algorithm

4.2 The sech-squared function

In order to illustrate the influence of the parameter χ on the SCSA, we first study a sech-squared function given by

$$y(t) = \operatorname{sech}^2(t - t_0), \quad x \in \mathbb{R}. \tag{38}$$

The potential of the Schrödinger operator $H_1(\chi y)$ is given in this case by: $-\chi \operatorname{sech}^2(t - t_0)$. This potential is called in quantum physics *Pöschl–Teller* potential.

It is well-known that the *Pöschl–Teller* potential belongs to the class of reflectionless potentials if,

$$\chi = \chi_p = N(N+1), \quad N = 1, 2, 3, \ldots, \tag{39}$$

N being the number of negative eigenvalues of $H_1(\chi y)$ [22].

So, for example, if $\chi = 2$, the Schrödinger operator spectrum is negative and consists of a single negative eigenvalue given by $\lambda = -1$. If $\chi = 6$, there are two negative eigenvalues: $\lambda_1 = -4$, $\lambda_2 = -1$ and so on.

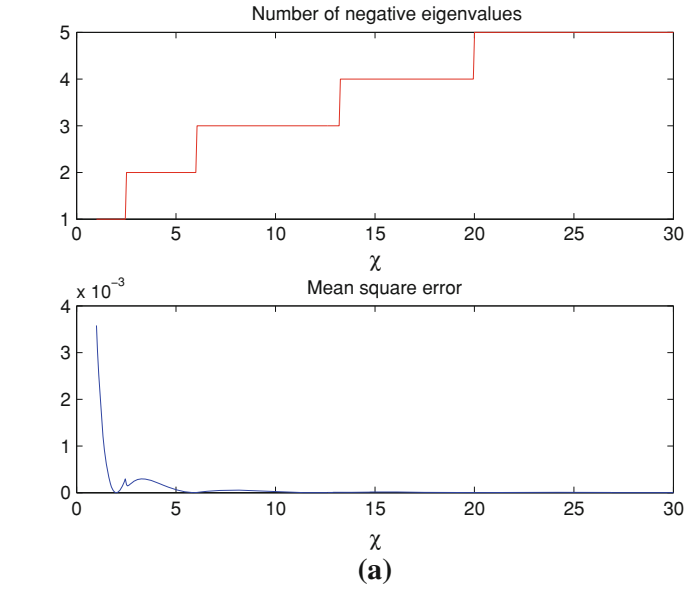

(a)

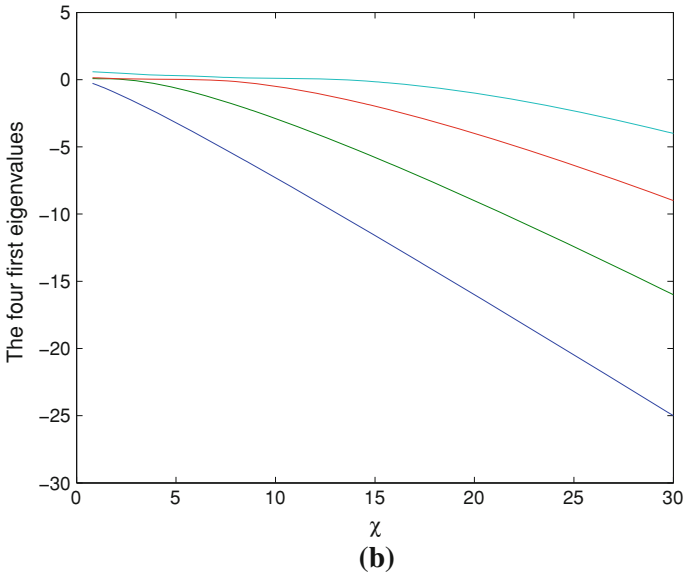

(b)

Fig. 3 **a** Mean square error and number of negative eigenvalues according to χ for $y(t) = \text{sech}^2(t-6)$ in $[0, 15]$. **b** Four first eigenvalues according to χ for $y(t) = \text{sech}^2(t-6)$ in $[0, 15]$

Let us now apply the SCSA to reconstruct y. For this purpose, we must truncate the signal and consider it on a finite interval so that the numerical computations could be possible.

Figure 3a illustrates the variation of the mean square error and N_χ according to χ. We notice that,

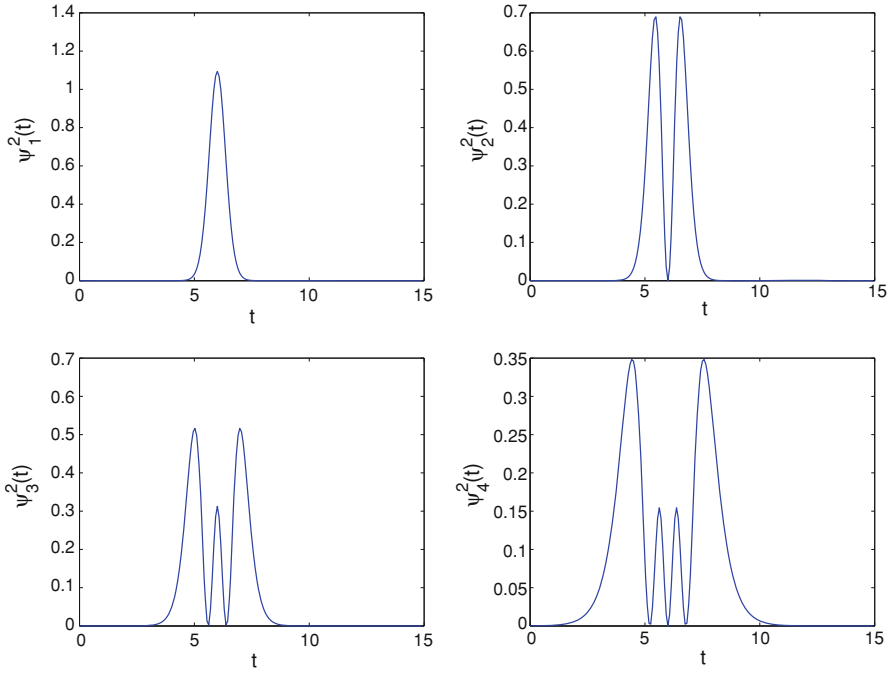

Fig. 4 Four first eigenfunctions $\psi^2_{n\chi}$ for $\chi = 20$ for $y(t) = \text{sech}^2(t-6)$ in $[0, 15]$

- N_χ is an increasing function of χ as described in proposition (1). Moreover, N_χ is a step-by-step function.
- There are some particular values of χ for which the error is minimal. These values are in fact the particular values $\chi_p = N_\chi(N_\chi + 1)$, $N_\chi = 1, 2, \ldots$ for which $-\chi y$ is a reflectionless potential.
- For all $\epsilon > 0$, there is a value $\chi = \chi_\epsilon$ such that $\forall \chi > \chi_\epsilon, \quad J(\chi) < \epsilon$.

Figure 3b illustrates the variation of the first four eigenvalues of the matrix $-\boldsymbol{D}_2 - \chi\,\text{diag}(\boldsymbol{Y})$, settled in an increasing way, according to χ. We notice that these eigenvalues, initially positive, are decreasing functions of χ and at every passage from N_χ to $N_\chi + 1$, a positive eigenvalue becomes negative.

Otherwise, in Fig. 4, the first four squared eigenfunctions $\psi^2_{n\chi}$, $n = 1, \ldots, 4$ are represented for $\chi = 20$. Each $\psi^2_{n\chi}$ has $n - 1$ zeros.

Figure 5 shows a satisfactory reconstruction of y for $N_\chi = 1, 2, 3$ and 4.

4.3 Estimation of some signals

In this section, we are interested in the estimation of some signals with the SCSA. In each case, we represent the estimation error, the number of negative eigenvalues according to χ and the real and estimated signals for different values of χ.

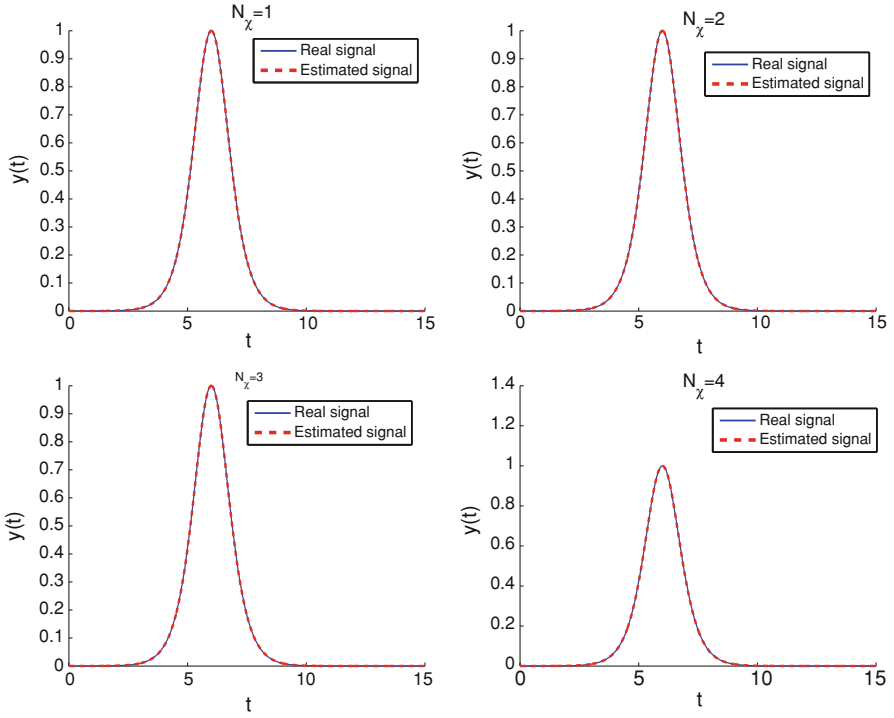

Fig. 5 Estimation of $y(t) = \text{sech}^2(t-6)$ in $[0, 15]$, from the left to the right $N_\chi = 1$, $N_\chi = 2$ (*top*). $N_\chi = 3$, $N_\chi = 4$ (*bottom*)

We start with a gaussian signal given by:

$$y(t) = \frac{1}{\sigma\sqrt{2\pi}} e^{-\frac{(t-\mu)^2}{2\sigma^2}}. \tag{40}$$

For the numerical tests we take $\sigma = 0.1$ and $\mu = 0.75$.

Figures 6 and 7 illustrate the results. We notice that with $N_\chi = 2$, the estimation is satisfactory and as N_χ increases better is the approximation.

Now we are interested in a sinusoidal signal defined in a finite interval I,

$$y(t) = \begin{cases} A\sin(\omega t + \phi) & t \in I \\ 0 & \text{otherwise} \end{cases} \tag{41}$$

This signal has negative values, so to apply the SCSA, we must translate the signal by $y_{\min} = -A$ such that $y - y_{\min} > 0$. The Schrödinger operator potential to be considered is then given by $-\chi(y - y_{\min})$. For the numerical tests, we took $A = 2$, $\omega = \pi$ and $\phi = -0.5$.

The results are represented in Figs. 8, 9 and 10. In 9, a single period of the signal is considered while in 10, four periods are represented. In the last case we noticed that the negative eigenvalues are of multiplicity 4, they are repeated in each period.

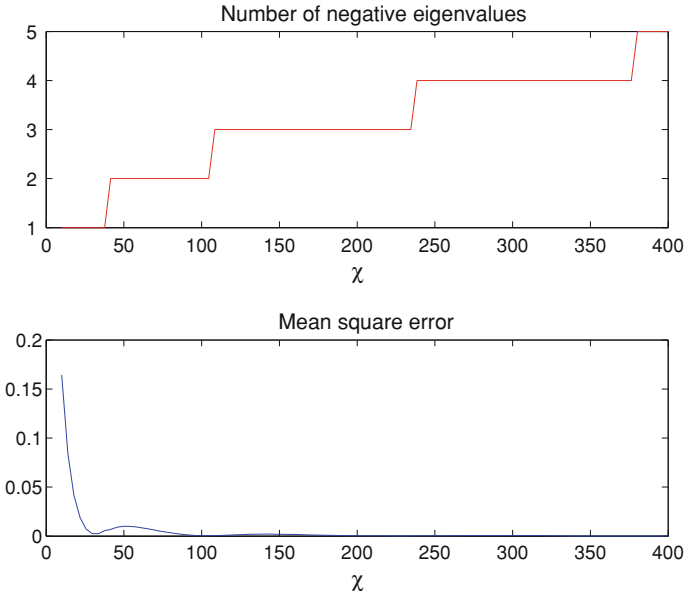

Fig. 6 Mean square error and number of negative eigenvalues according to χ for a gaussian signal

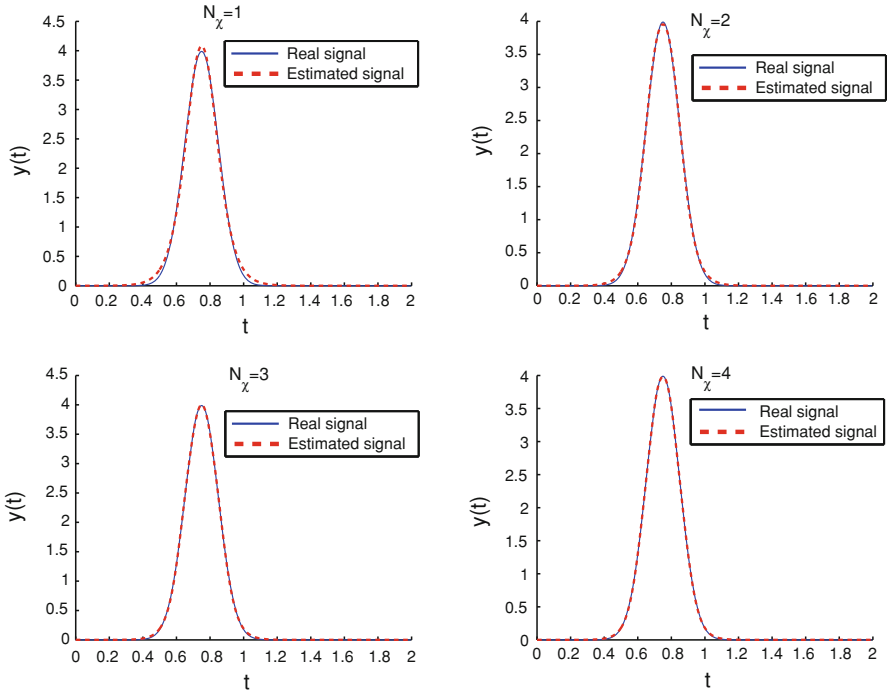

Fig. 7 Estimation of a gaussian signal, *from the left to the right* $N_\chi = 1$, $N_\chi = 2$ (*top*). $N_\chi = 3$, $N_\chi = 4$ (*bottom*)

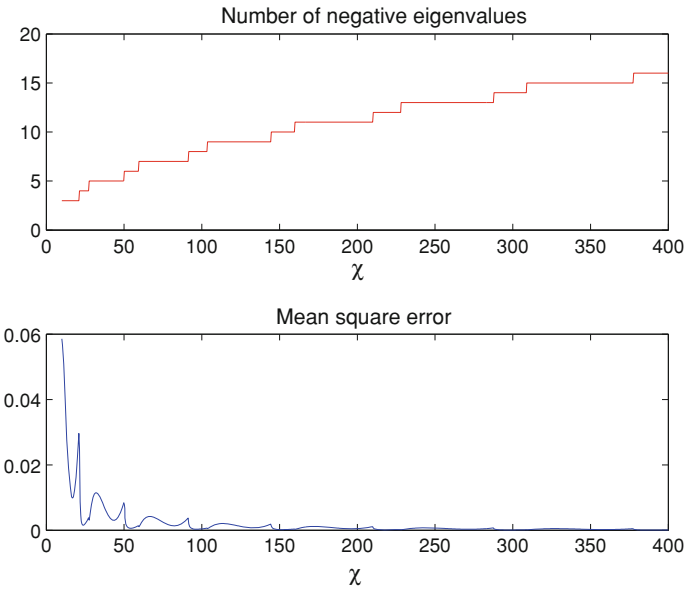

Fig. 8 Mean square error and number of negative eigenvalues according to χ for a sinusoidal signal

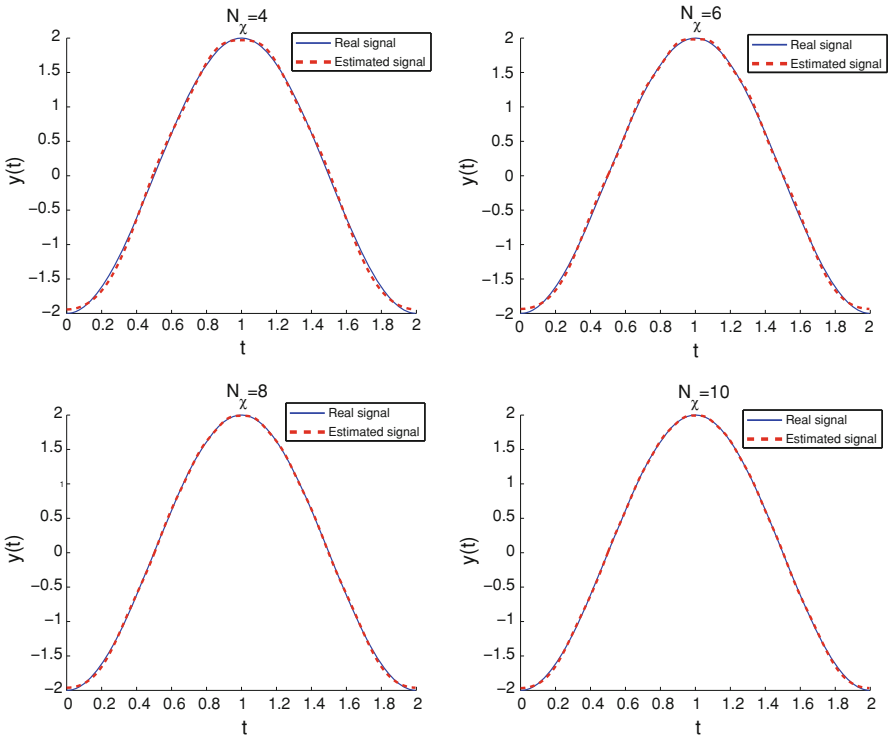

Fig. 9 Estimation of a sinusoidal signal, *from the left to the right* $N_\chi = 4$, $N_\chi = 6$ (*top*). $N_\chi = 8$, $N_\chi = 10$ (*bottom*)

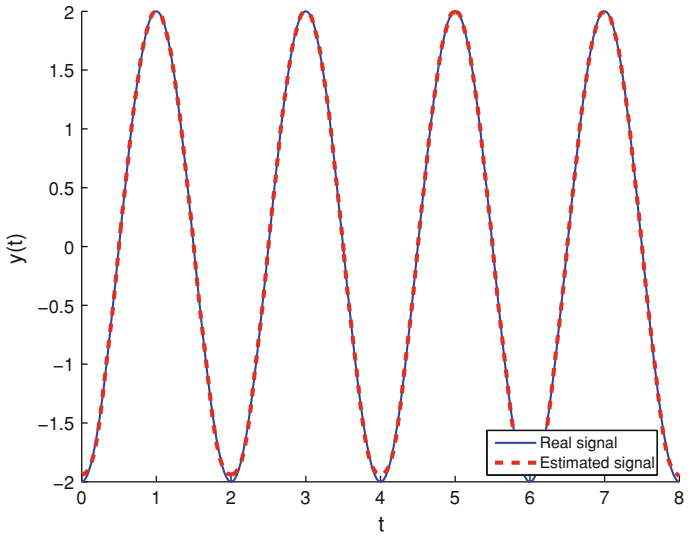

Fig. 10 Estimation of 4 sinusoidal signal periods with $N_\chi = 10$

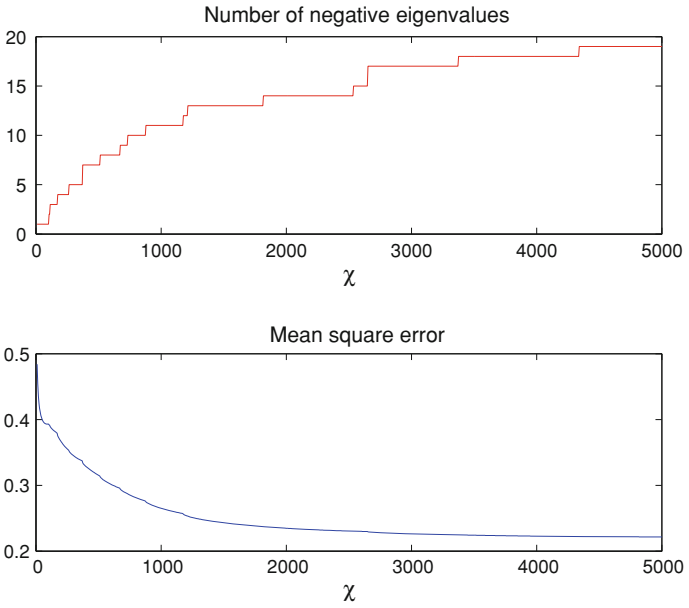

Fig. 11 Mean square error and number of negative eigenvalues according to χ for a chirp signal

Finally, Figs. 11 and 12 illustrate the results obtained in the case of a chirp signal. We recall that a chirp signal is usually defined by a time varying frequency sinusoid. In our tests, we considered a linear variation of the frequency.

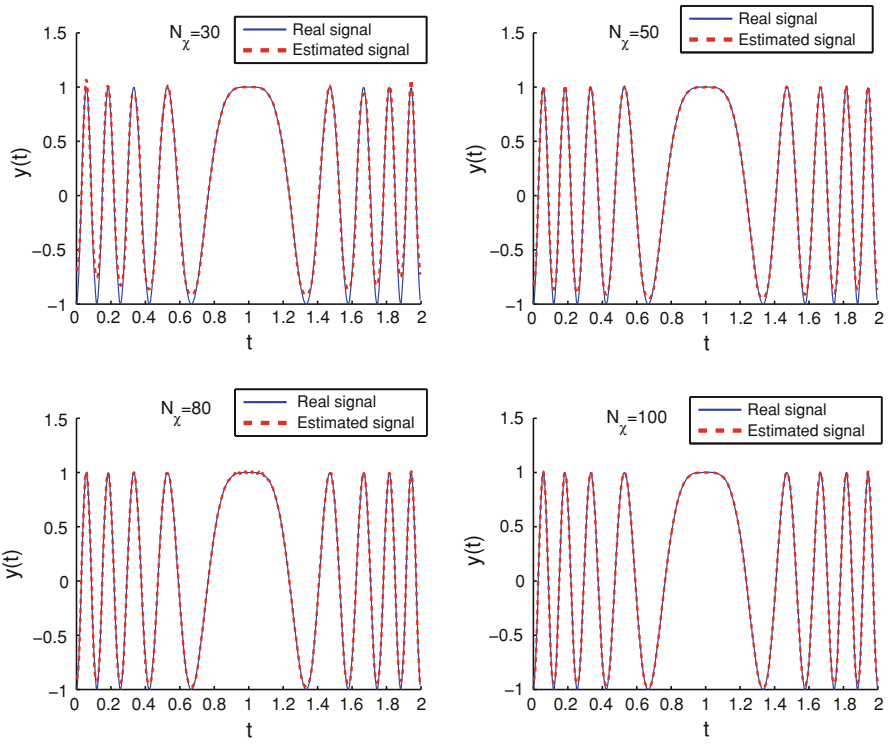

Fig. 12 Estimation of a chirp signal, *from the left to the right* $N_\chi = 30$, $N_\chi = 50$ (*top*). $N_\chi = 80$, $N_\chi = 100$ (*bottom*)

5 Arterial blood pressure analysis with the SCSA

ABP plays an important role in the cardiovascular system. So many studies were done aiming at proposing mathematical models in order to understand the cardiovascular system both in healthy and pathological cases. Despite the large number of ABP models, the interpretation of ABP in clinical practice is often restricted to the interpretation of the maximal and the minimal values called respectively the systolic pressure and the diastolic pressure. None information on the instantaneous variability of the pressure is given in this case. However, pertinent information can be extracted from ABP waveform. The SCSA seems to provide a new tool for the analysis of ABP waveform. This section presents some obtained results.

We denote the ABP signal P and $\hat{P}$ its estimation using the SCSA such that

$$\hat{P}(t) = \frac{4}{\chi} \sum_{n=1}^{N_\chi} \kappa_{n\chi} \psi_{n\chi}^2(t), \tag{42}$$

where $-\kappa_{n\chi}^2, n = 1, \ldots, N_\chi$ are the N_χ negative eigenvalues of $H_1(\chi P)$ and $\psi_{n\chi}$ the associated L^2-normalized eigenfunctions.

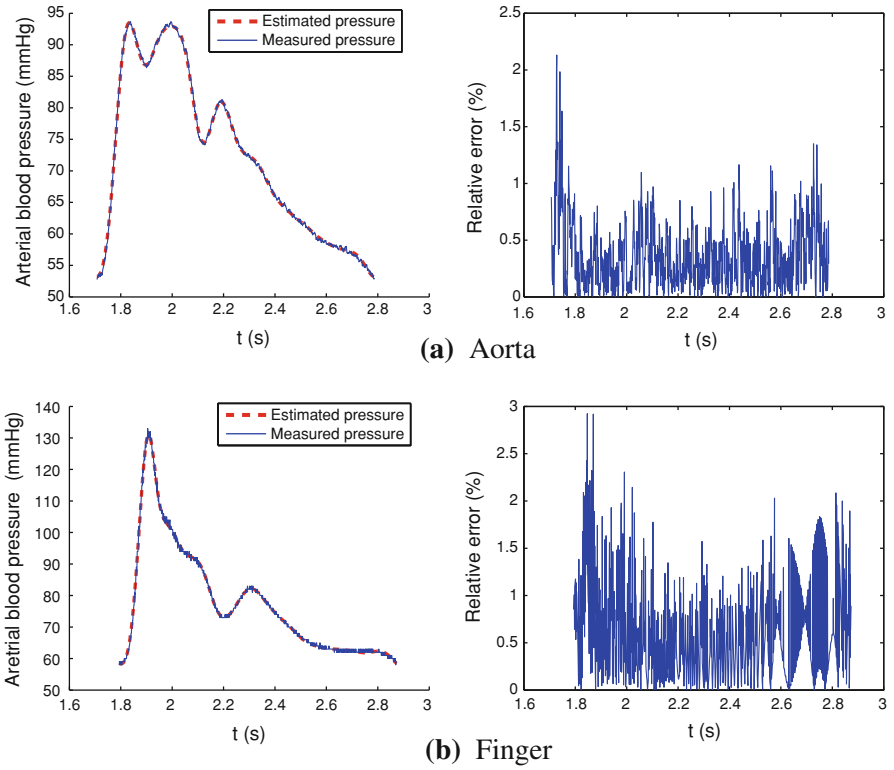

Fig. 13 Reconstruction of the pressure at the aorta and the finger level with the SCSA and $N_\chi = 9$. On the *left* the estimated and measured pressures, on the *right* the relative error

The ABP signal was estimated for several values of the parameter χ and hence N_χ. Figure 13 illustrates the measured and estimated pressures for one beat of ABP and the estimated error with $N_\chi = 9$. Signals measured at the aorta level and the finger respectively were considered. We point out that 5–9 negative eigenvalues are sufficient for a good estimation of ABP signals [17,19].

A first interest in using the SCSA for ABP analysis is to decompose the signal into its systolic and diastolic parts, respectively. This application was inspired from a reduced model of ABP based on solitons introduced in [4,18]. Solitons are in fact solutions of some nonlinear partial derivative equations for instance the Korteweg-de Vries (KdV) equation which was considered in this reduced model [4]. This model proposes ABP as the sum of two terms: N-soliton, solution of the KdV equation describing fast phenomena that predominate during the systolic phase and a two-element windkessel model that describes slow phenomena during the diastolic phase. Moreover, the KdV equation can be solved with the Inverse Scattering Transform (IST) whose definition is recalled in Appendix Appendix A:. In this approach, the KdV equation is associated to a one-dimensional Schrödinger potential parameterized by time where the potential is given by the solution of the KdV equation at a given time. Therefore, a relation between the Schrödinger operator and solitons was found [10]; solitons are reflection-

less potentials. Then according to Proposition 4, the SCSA coincides with a soliton representation of a signal for a finite χ when $-\chi y$ is an N_χ-soliton, where N_χ denotes the number of negative eigenvalues[1] of $H_1(\chi y)$. So each spectral component represents a single soliton. We know that solitons are characterized by their velocity which is determined by the negative eigenvalues $-\kappa_{n\chi}^2$, $n = 1, \ldots, N_\chi$ of the Schrödinger operator. The largest values $\kappa_{n\chi}$ characterize fast components and the small values of $\kappa_{n\chi}$ characterize slow components. From these remarks, we propose to decompose Eq. (31) into two partial sums: the first one, composed of the N_s ($N_s = 1, 2, 3$ in general) largest $\kappa_{n\chi}$ and the second partial sum composed of the remaining components. The first partial sum describes the systolic phase and the second one describes the diastolic phase. We denote $\hat{P}_s$ and $\hat{P}_d$ the systolic pressure and the diastolic pressure, respectively estimated with the SCSA. Then, we have

$$\hat{P}_s(t) = \frac{4}{\chi} \sum_{n=1}^{N_s} \kappa_{n\chi} \psi_{n\chi}^2(t), \qquad \hat{P}_d(t) = \frac{4}{\chi} \sum_{n=N_s+1}^{N_\chi} \kappa_{n\chi} \psi_{n\chi}^2(t). \tag{43}$$

Figure 14 represents the measured pressure and the estimated systolic and diastolic pressures, respectively. We notice that $\hat{P}_s$ and $\hat{P}_d$ are respectively localized during the systole and the diastole.

6 Discussion

The spectral analysis of the Schrödinger operator introduces two inverse problems: an inverse spectral problem and an inverse scattering problem.

On the one hand, the inverse spectral problem aims at reconstructing the potential of a Schrödinger operator with its spectrum (spectral function). It has been extensively studied for instance by Borg, Gel'Fand, Levitan and Marchenko [11] or more recently by Ramm [27]. They considered the half-line case and used two spectra of the Schrödinger operator with two different boundary conditions in order to reconstruct the potential. The inverse spectral problem for a semi-classical Schrödinger operator $H_h(y)$ have been recently considered for example by Colin de Verdiére [5] who proposed to reconstruct the potential locally with a single spectrum or Guillemin and Uribe [13] who showed that under some assumptions, the low-lying eigenvalues of the operator determine the Taylor series of the potential at the minimum.

In this work, we have studied an inverse spectral approach that is different from classical inverse spectral problems. Indeed, we used more information to reconstruct the potential by including the eigenfunctions as illustrated by Eq. (3).

On the other hand, the inverse scattering problem aims at recovering the potential from the scattering data (see Appendix Appendix A:). Many studies considered this question for instance those of Marchenko [25] who proved that under some conditions on the scattering data, a potential in $L_1^1(\mathbb{R})$ can be reconstructed from these scattering data and gave an algorithm for recovering the potential. We can also quote works

[1] Each soliton is characterized by a negative eigenvalue.

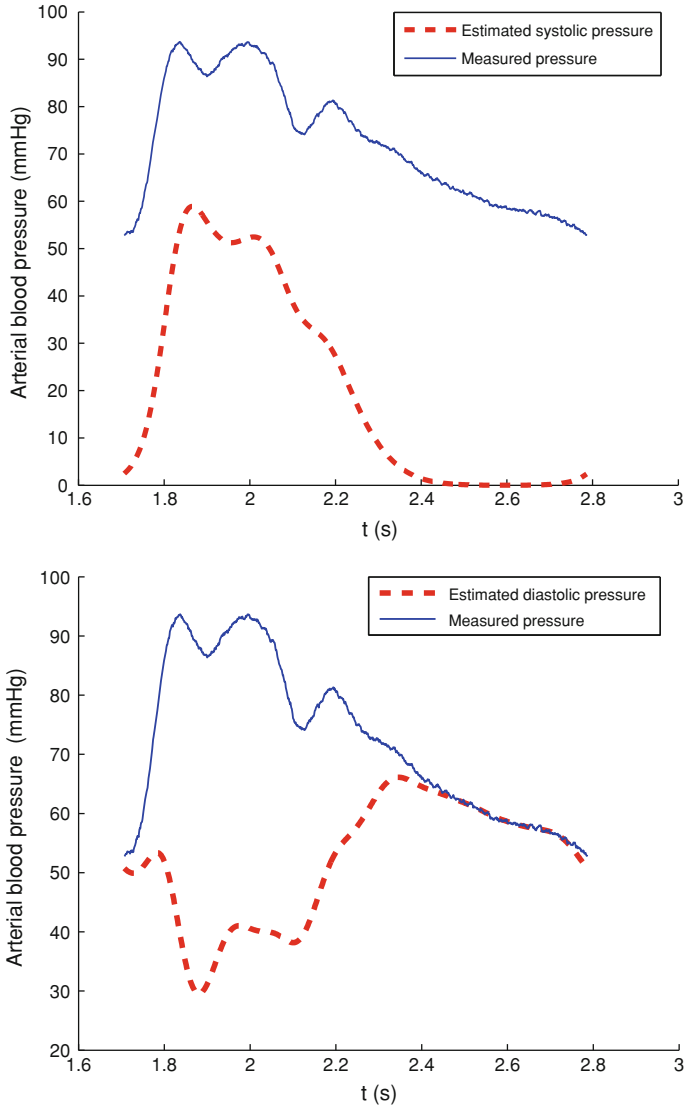

Fig. 14 On the *left* the estimated systolic pressure. On the *right* estimated diastolic pressure

of Faddeev [9], Deift and Trubowitz [6] considering potentials in $L^1_1(\mathbb{R})$, Dubrovin, Matveev and Novikov [7] for periodic potentials.

The convergence of the SCSA when $h \to 0$ is not easy to study. Using the Deift-Trubowitz formula (52), we have tried to consider this problem. However, despite interesting results obtained regarding the convergence of some quantities depending only on the continuous spectrum of the Schrödinger operator to zero, we did not succeed in finding a result of convergence for y_h. A study supported by semi-classical concepts is now under consideration. The latter is based on the generalization of the results of G. Karadzhov [16].

The SCSA method has given promising results in the analysis of arterial blood pressure waveforms. More than a good reconstruction of these signals, the SCSA introduces interesting parameters that give relevant physiological information. These parameters are the negative eigenvalues and the invariants which are given by the momentums of $\kappa_{n\chi}$, $n = 1, \ldots, N_\chi$ introduced in Proposition 3. For example, these new cardiovascular indices allow the discrimination between healthy patients and heart failure subjects [21]. A recent study [20] shows that the first systolic momentum (associated to the systolic phase) gives information on stroke volume variation, a physiological parameter of great interest.

We have seen in Proposition 4 that for a fixed value of h the SCSA coincides with a reflectionless potentials approximation. This point seems to be an interesting avenue of research. Indeed, thanks to the relation between reflectionless potentials and solitons, the approximation by reflectionless potentials could have interesting applications in signal analysis and in particular in data compression. As we said in the previous section, solitons are reflectionless potentials of the Schrödinger operator. Gardner et al [10] showed that an N-soliton is completely determined by the discrete scattering data and in particular by $2N$ parameters which are the negative eigenvalues and the normalizing constants. Hence, if $-\chi y$ is an N_χ-soliton, it is given by the following formula:

$$y(t) = \frac{2}{\chi}\frac{\partial^2}{\partial t^2}\ln\left(\det\left(I + A_\chi\right)\right)(t), \quad x \in \mathbb{R}, \tag{44}$$

$A_\chi(t)$ is an $N_\chi \times N_\chi$ matrix of coefficients

$$A_\chi(t) = \left[\frac{c_{m\chi}c_{n\chi}}{\kappa_{m\chi}+\kappa_{n\chi}}e^{-(\kappa_{m\chi}+\kappa_{n\chi})x}\right]_{n,m}, \quad n, m = 1, \ldots, N_\chi, \tag{45}$$

where $-\kappa_{n\chi}^2$ and $c_{n\chi}, n = 1, \ldots, N_\chi$ are the negative eigenvalues and the normalizing constants of $H_1(\chi y)$. Hence, this formula provides a parsimonious representation of a signal.

The convergence of the approximation by solitons (or reflectionless potentials) when $\chi \to +\infty$ (equivalently $h \to 0$) was studied by Lax and Levermore [24] in a different context. Indeed they studied the small dispersion limit of the KdV equation and approached the initial condition of the KdV equation by an N-soliton that depends on the small dispersion parameter which is in our case h. They showed the results in the mono-well potential case and affirmed without proving that the result still remains true for multi-well potentials. However, the main limitation of this approach is the difficulty to compute the normalizing constants. This difficulty can be explained by the fact that these constants are defined at infinity which cannot be handled in the numerical implementation. At the best of our knowledge there is no study enabling the computation of these parameters apart a recent attempt by Sorine et al. [29].

7 Conclusion

A new method for signal analysis based on a semi-classical approach has been proposed in this study: the signal is considered as a potential of a Schrödinger operator and then

represented using the discrete spectrum of this operator. Some spectral parameters are then computed leading to a new approach for signal analysis. This study is a first step in the validation of the SCSA. Indeed, we have assessed here the ability of the SCSA to reconstruct some signals. We have studied particularly a challenging application which is the analysis of the arterial blood pressure waveforms. The SCSA introduces a novel approach for arterial blood pressure waveform analysis and enables the estimation of relevant physiological parameters. A theoretical study is now under consideration regarding the convergence of the SCSA for $h \to 0$. The work must be orientated at a second step to the comparison between the performance of the SCSA and other signal analysis methods like Fourier transform or the wavelets and also to the generalization of the SCSA to other fields.

Acknowledgments The authors thank Doctor Yves Papelier from the Hospital Béclère in Clamart for providing us arterial blood pressure data.

Appendix A: Direct and inverse scattering transforms

These appendices recall some known concepts on direct and inverse scattering transforms of a one-dimensional Schrödinger operator. For more details, the reader can refer to the large number of references on this subject for instance [1,3,6,8,9]. Note that in this appendix we used the usual notations, in particular the variable here is x and not t.

We consider here the spectral problem of a Schrödinger operator $H_1(-V)$, given by

$$-\frac{d^2\psi}{dx^2} + V(x,t)\psi = k^2\psi, \quad k \in \overline{\mathbb{C}}^+, \quad x \in \mathbb{R}, \tag{46}$$

where the potential V such that $V \in \mathcal{B}$. For simplicity, we will omit the indice 1 of the spectral parameters in the following.

For $k^2 > 0$, we introduce the solutions $\psi_\pm$ of Eq. (46) such that

$$\psi_-(k,x) = \begin{cases} T(k)e^{-ikx} & x \to -\infty, \\ e^{-ikx} + R_r(k)e^{+ikx} & x \to +\infty, \end{cases} \tag{47}$$

$$\psi_+(k,x) = \begin{cases} T(k)e^{+ikx} & x \to +\infty, \\ e^{+ikx} + R_l(k)e^{-ikx} & x \to -\infty, \end{cases} \tag{48}$$

where $T(k)$ is called the transmission coefficient and $R_{l(r)}(k)$ are the reflection coefficients from the left and the right, respectively. The solution ψ_- for example describes the scattering phenomenon for a wave e^{-ikx} of amplitude 1, sent from $+\infty$. This wave hit an obstacle which is the potential so that a part of the wave is transmitted $T(k)e^{-ikx}$ and the other part is reflected $R_r(k)e^{+ikx}$. ψ_+ describes the scattering phenomenon for a wave e^{+ikx} sent from $-\infty$.

For $k^2 < 0$, the Schrödinger operator spectrum has N negative eigenvalues denoted $-\kappa_n^2$, $n = 1, \ldots, N$. The associated L^2-normalized eigenfunctions are such that

$$\psi_n(x) = c_{ln} e^{-\kappa_n x}, \qquad x \to +\infty, \tag{49}$$
$$\psi_n(x) = (-1)^{N-n} c_{rn} e^{+\kappa_n x}, \quad x \to -\infty, \tag{50}$$

c_{ln} and c_{rn} are the normalizing constants from the left and the right, respectively.

The spectral analysis of the Schrödinger operator introduces two transforms:

- The direct scattering transform (DST) which consists in determining the so-called scattering data for a given potential. Let us denote $\mathcal{S}_l(V)$ and $\mathcal{S}_r(V)$ the scattering data from the left and the right, respectively:

$$\mathcal{S}_j(V) := \{R_{\overline{j}}(k),\ \kappa_n,\ c_{jn},\ \ n = 1, \ldots, N\}, \qquad j = l, r, \tag{51}$$

  where $\overline{j} = r$ if $j = l$ and $\overline{j} = l$ if $j = r$.
- The inverse scattering transform (IST) that aims at reconstructing a potential V using the scattering data.

The scattering transforms have been proposed to solve some partial derivative equations for instance the KdV equation [10].

Appendix B: Reflectionless potentials

Deift and Trubowitz [6] showed that when the Schrödinger operator potential V satisfies hypothesis (2), then it can be reconstructed using an explicit formula given by

$$V(x) = -4 \sum_{n=1}^{N} \kappa_n \psi_n^2(x) + \frac{2i}{\pi} \int_{-\infty}^{+\infty} k R_{r(l)}(k)\ f_{\pm}^2(k, x) dk, \quad x \in \mathbb{R}. \tag{52}$$

This formula is called the *Deift-Trubowitz trace formula*. It is given by the sum of two terms: a sum of $\kappa_n \psi_n^2$ that characterizes the discrete spectrum, and an integral term that characterizes the contribution of the continuous spectrum.

There is a special class of potentials called reflectionless potentials for which the problem is simplified. A reflectionless potential is defined by $R_{l(r)}(k) = 0, \forall k \in \mathbb{R}$. According to the Deift-Trubowitz formula, a reflectionless potential can be written using the discrete spectrum only,

$$V(x, t) = -4 \sum_{n=1}^{N} \kappa_n \psi_n^2(x, t), \tag{53}$$

Appendix C: An infinite number of invariants

There is an infinite number of time invariants for the KdV equation given by the conserved quantities [10,12,26]. Let us denote these invariants $I_m(V)$, $m = 0, 1, 2, \ldots$. They are of the form

$$I_m(V) = (-1)^{m+1} \frac{2m+1}{2^{2m+2}} \int_{-\infty}^{+\infty} P_m \left(V, \frac{\partial V}{\partial x}, \frac{\partial^2 V}{\partial x^2}, \cdots \right) dx, \tag{54}$$

where $P_m, m = 0, 1, 2, \ldots$ are known polynomials in V and its successive derivatives with respect to $x \in \mathbb{R}$ [3].

A general formula relates $I_m(V)$ to the scattering data of $H_1(-V)$ [3,12,26] as follows:

$$I_m(V) = \sum_{n=1}^{N} \kappa_n^{2m+1} + \frac{2m+1}{2\pi} \int_{-\infty}^{+\infty} (-k^2)^m \ln\left(1 - |R_{r(l)}(k)|^2\right) dk, \tag{55}$$

$m = 0, 1, 2, \ldots$. So, for $m = 0$, $P_0(V, \cdots) = V$, we get with (54) and (55):

$$\int_{-\infty}^{+\infty} V(x) dx = -4 \sum_{n=1}^{N} \kappa_n - \frac{1}{\pi} \int_{-\infty}^{+\infty} \ln\left(1 - |R_{r(l)}(k)|^2\right) dk. \tag{56}$$

References

1. Aktosun T, Klaus M (2001) Inverse theory: problem on the line. Academic Press, London ch.2.2.4 770–785
2. Blanchard Ph, Stubbe J (1996) Bound states for Schrödinger Hamiltonians: phase space methods and applications. Rev Math Phys 35:504–547
3. Calogero F, Degasperis A (1982) Spectral transform and solitons, vol 1, North-Holland publishing company, Amsterdam
4. Crépeau E, Sorine M (2007) A reduced model of pulsatile flow in an arterial compartment. Chaos Solitons Fractals 34:594–605
5. Colin de Verdire Y (2008) A semi-classical inverse problem II: reconstruction of the potential. Preprint
6. Deift PA, Trubowitz E (1979) Inverse scattering on the line. Comm Pure appl Math XXXII:121–251
7. Dubrovin PA, Matveev VB, Novikov SP (1976) Nonlinear equations of Korteweg-de Vries type, finite-zone linear operators, and Abelian varieties. Russian Math Surv 31:59–146
8. Eckhaus W, Vanharten A (1981) The inverse scattering transformation and the theory of solitons, vol 50, North-Holland publishing company, Amsterdam
9. Faddeev LD (1964) Properties of the S-matrix of the one-dimensional Schrdinger equation. Trudy Mat Inst Steklov 73:314–336
10. Gardner CS, Greene JM, Kruskal MD, Miura RM (1974) Korteweg-de Vries equation and generalizations VI. Methods for exact solution. In: Communications on Pure and Applied Mathematics, vol XXVII. J Wiley & sons, New York, pp 97–133
11. Gel'fand IM, Levitan BM (1955) On the determination of a differential equation from its spectral function. Am Math Soc Transl 2:253–304
12. Gesztesy F, Holden H (1994) Trace formulas and conservation laws for nonlinear evolution equations. Rev Math Phys 6:51–95
13. Guillemin V, Uribe A (2005) Some inverse spectral results for semi-classical schrödinger operators. Preprint
14. Helffer B, Robert D (1990) Riesz means of bound states and semiclassical limit connected with a Lieb-Thirring's conjecture I. Asymptot Anal 3:91–103
15. Hussaini MY, Gottlieb D and Orszag SA (1984) Theory and applications of spectral methods. In: Gottlieb D, Voigt R, Hussaini M (eds) Spectral methods for partial differential equations, pp 1–54
16. Karadzhov G (1990) Asymptotique semi-classique uniforme de la fonction spectrale d'opérateurs de Schrödinger. C R Acad Sci Paris, t. 310, Série I:99–104

17. Laleg TM, Crépeau E, Papelier Y, Sorine M (2007) Arterial blood pressure analysis based on scattering transform I. In: Proc. EMBC Sciences and Technologies for Health Lyon France
18. Laleg TM, Crépeau E, Sorine M (2007) Separation of arterial pressure into a nonlinear superposition of solitary waves and a windkessel flow. Biomed Signal Process Control J 2:163–170
19. Laleg TM, Crépeau E, Sorine M (2007) Travelling-wave analysis and identification. A scattering theory framework. In: Proc, European Control Conference ECC Kos Greece
20. Laleg TM, Médigue C, Papelier Y, Cottin F, Van de Louw (submitted) A Validation of a new method for stroke volume variation assessment: a comparison with the picco technique. http://arxiv.org/PS_cache/arxiv/pdf/0911/0911.0837v3.pdf
21. Laleg TM, Médigue C, Cottin F and Sorine M (2007) Arterial blood pressure analysis based on scattering transform II. In: Proc. EMBC Lyon France
22. Landau LD, Lifshitz EM (1958) Quantum mechanics: non-relativistic theory, vol 3. Pergamon Press, Oxford
23. Laptev A, Weidl T (2000) Sharp Lieb-Thirring inequalities in high dimensions. Acta Math 184:87–111
24. Lax PD, Levermore CD (1983) The small dispersion limit of the Korteweg-de Vries equation I, II, III. Comm Pure appl Math 36:253–290, 571–593, 809–828
25. Marchenko VA (1986) Sturm-Liouville operators and applications. Birkhuser Basel
26. Molchanov S, Novitskii M, Vainberg B (2001) First KdV integrals and absolutely continuous spectrum for 1-d Schrodinger operator. Commun Math Phys 216:195–213
27. Ramm AG (1998) A new approach to the inverse scattering and spectral problems for the strum-liouville equation. Annal der Physik 7:321–338
28. Reed M, Simon B (1978) Methods of modern mathematical physics IV. Analysis of operators theory. Academic Press, New York
29. Sorine M, Zhang Q, Laleg TM, Crepeau E (2008) Parsimonious representation of signals based on scattering transform. In: IFAC'08
30. Trefethen LN (2000) Spectral Methods in Matlab. SIAM